Monotonic characterisation of low- to medium-density chalk for driven offshore pile design

K. Vinck
Imperial College London, London, UK

T. Liu
University of Bristol, Bristol, UK

R.J. Jardine
Imperial College London, London, UK

S. Kontoe
University of Patras, Patras, Greece

R.M. Buckley
University of Glasgow, Glasgow, UK

B.W. Byrne
University of Oxford, Oxford, UK

R.A. McAdam
Ørsted Power Ltd, London, UK

P. Ferreira, M. Coop
University College London, London, UK

ABSTRACT: Driven piles support a substantial number of offshore wind turbines, near-shore bridges, and port facilities. Designing and installing these piles can be challenging in Chalk, a porous, low-density, weak carbonate rock prevalent beneath vast areas of NW Europe. Designers currently have limited guidance on driveability, axial capacity, lateral pile resistance - a key factor in offshore wind turbine monopile behaviour, and how these piles can endure axial or lateral cyclic loading. This paper outlines the characterisation of very weak to weak, low- to medium-density chalk via in situ profiling and laboratory testing. The experimental characterisation identified chalk behaviour traits that demand meticulous consideration in numerical analysis for modelling real-world issues, including chalk's noticeable sensitivity, brittleness, pressure dependency, anisotropy, and strain rate dependency. These findings formed the groundwork for numerical analysis using advanced constitutive models to aid in interpreting axial and lateral tests on driven piles.

1 **Introduction**

Underlying vast expanses of North-West Europe, the Middle East, and other regions is Chalk, a highly inconsistent soft cemented biomicrite limestone. This presents a variety of problems for geotechnical engineers (Mortimore, 2012). Chalks with several MPa of unconfined compressive strengths (UCS) can maintain stability in moderately tall coastal cliffs. However, reliably evaluating its reaction to foundation loading is challenging due to its propensity for fissuring, brittleness, and sensitivity. During pile driving, chalk is 'de-structured' beneath the advancing pile tips and around their shafts, creating thin 'putty' annuli around their shafts (Lord et al., 2022). These attributes create significant uncertainty about driving resistances and both monotonic and cyclic, axial and lateral capacities at different stages of aging. Furthermore, it's been shown by recent offshore North and Baltic Sea wind energy projects that the current guidelines are inadequately reliable for ensuring safe and economically feasible design of driven piles in chalk (Barbosa et al., 2017 and Buckley et al., 2020).

To ensure safe and efficient design for offshore wind and other onshore or near-shore projects, it's vital to allow a more representative characterisation of the piles' response to axial and lateral, monotonic and cyclic, loading. This goal was progressed through the ALPACA and ALPACA Plus Joint Industry Projects (JIPs). They examined the behaviour of 41, primarily instrumented, tubular steel piles under dynamic, axial and lateral, monotonic and cyclic loading at the St Nicholas-at-Wade (SNW) (Kent, UK) research site (Jardine et al., 2023a).

This paper offers a summarised view of key findings from advanced in situ and laboratory testing carried out for ALPACA on intact low- to medium-density SNW chalk, as reported by Vinck (2021), Vinck et al. (2022) and Liu et al. (2023a). The fieldwork incorporated multiple cone penetration tests (CPT), pressuremeter profiling, sampled boreholes, and a large sampling pit. The extensive laboratory programme included index and oedometer profiling and over 100 advanced tests using locally instrumented, automated stress path triaxial equipment that investigated the intact chalk's mechanical behaviour, as well as its anisotropic and yielding features in tests that ranged from comparatively low in-situ stress circumstances to high pressures imposing p_0' up to 12.8 MPa.

The testing covered both intact and de-structured chalk. Jardine et al. (2023b) establish that the performance of piles driven in chalk under monotonic and cyclic axial loading is dictated by the behaviour of the chalk putty that forms during pile driving, as manifested after reconsolidation to long-term pile shaft

effective stress conditions. However, it's demonstrated by McAdam et al. (2022) and Pedone et al. (2022) that the piles' response to monotonic lateral loading is primarily governed by the brittle and fractured chalk surrounding the putty zone. The piles' reaction to repetitive lateral loading is also governed by the cyclic response of 'intact' chalk that experienced further fracturing during pile driving.

The cyclic loading triaxial experiments conducted for ALPACA are separately reported. Ahmadi-Naghadeh et al. (2022) study intact chalk's cyclic behaviour, while Liu et al. (2022) examine reconsolidated putty-like chalk under comparable stresses. Liu et al. (2023b) further interpret these tests, demonstrating their application in evaluating axial cyclic loading's impact on chalk site pile design.

2 **Field characterisation and in situ testing**

Vinck (2021) outlines the stratigraphy and structure of the pure white Margate and Seaford Chalk found at SNW, highlighting only minor weathering near the ground level. The Chalk is classified as CIRIA grade B3/B2 (structured, very weak to weak, low-to-medium density) within the depth of interest. Micro-fissures, primarily oriented vertically, were observed at 10 to 25 mm spacings at all depths.

Vinck et al. (2022) provide details on the typical index properties, seismic CPT profiles, and cone push-in pressuremeter results. Corrected cone resistances varied between 5 and 35 MPa, with higher resistances observed in thin, distinct flint bands. High pore water pressures ($\approx$ 4 MPa) were recorded at u_2 (shoulder) CPTu locations as the chalk began to destructure; the friction sleeve data displayed resistances dropping to 0.05 to 1 MPa as the chalk moved past the cone tips.

Index property measurements indicate low-density chalk with an intact dry density (IDD) ranging from 1.43 to 1.53 Mg/m^3, an average liquidity index of 0.91, and a degree of saturation that rose from $\approx$ 0.85 near the ground surface to $\approx$ 0.97 just above the water table and $\approx$ 1.00 below it.

3 **Mechanical laboratory tests**

The study on intact monotonic laboratory testing centred on specimens created from three 16m deep, Geobore-S wireline triple barrel rotary boreholes and eighteen 350 × 350 × 250mm blocks obtained from a 7m × 10m, 4m deep excavation. Efforts were made to mobilise, wherever feasible, pre-existing fissures and predominantly horizontal bedding planes during the meticulous block sampling process to minimise disturbance, steering clear of all visibly fractured material. Hand-tools and chainsaws were employed to separate blocks, which were immediately preserved in consecutive layers of foil, clingfilm, and wax. These blocks were then secured in plywood storage boxes with expanding polyurethane foam.

3.1 *Laboratory specimen preparation*

The meticulous preparation of chalk for mechanical test specimens in the laboratory is essential. Trials revealed that the use of plaster-of-Paris confining moulds and water-flush coring, with a highly stable radial-arm drill, is necessary to guarantee consistent production runs of high-quality specimens (Vinck 2021). The resulting cores were then contained in split aluminium moulds and then machined to meet the end flatness and parallelism tolerances set by ASTM (2019).

3.2 *Test equipment*

At Imperial College, triaxial testing was carried out using 38 mm diameter, 76 mm high specimens in computer-controlled Bishop and Wesley stress-path cells, rated for 4 MPa deviatoric stresses (q) and 750 kPa cell and back pressures. Additional experiments were conducted at University College London using GDS systems capable of administering significantly higher cell pressures and deviator stresses, q, up to 13 MPa to specimens that were 50 mm in diameter and 100 mm high. The equipment's functional capabilities, sensitivities, resolutions, and precisions are summarized by Vinck (2021) and Liu et al. (2023a), noting that local strain measurement was not feasible in the high-pressure tests.

3.3 *Triaxial testing procedures*

In the lab experiments, there was no attempt to mimic the complex sedimentary or post-sedimentary histories of chalk. Instead, isotropic consolidation stress paths were used. Accurate determination of in-situ K0 is challenging in chalk due to its typical systems of fissures, very high stiffness and sensitivity to disturbance caused by intrusive drilling. Despite the chalk's Cretaceous age and very high yield stress ratios a low K_0 = 0.6 was assumed (after Lord et al. 2002) when assessing in-situ stress conditions for laboratory testing. This was combined with unit weights and in-situ pore-pressure measurements from a deep piezometer and a tensiometer located above the water table $\approx$25 m away from the sampling pit area. Vinck et al. (2022) and Liu et al. (2023a) list the initial mean effective stresses p0′ from which drained (CID) and undrained (CIU) triaxial com-pression tests were undertaken to investigate the chalk's yielding in (compressive) triaxial effective stress-space.

Back pressures of 300 kPa and 900kPa were used for saturating specimens in low and high-pressure tests, respectively, until Skempton's (1954) pore pressure coefficient B consistently exceeded 0.95.

Subsequently, isotropic paths were travelled at 60 kPa/hour to the p_0' target. Higher-pressure tests utilized stages separated by 2-3 day pauses, allowing the associated volumetric strain to drop below 0.015% per day following pore pressure dissipation and creep. The CID tests followed an 5%/day external strain rate. System and load cell compliances caused local axial strain rates to be much lower until the chalk yielded.

4 Profiles of strength and stiffness

4.1 *Total stress peak shear strength*

Figure 1 depicts the peak deviator stress q_f and undrained shear strength s_u trends, revealing that the (jacketed) unconfined compression strength tests q_f values exceed those of the fully saturated triaxial tests by, on average, ≈ 22%. The higher UCS strengths reflect their specimens' generally higher effective stresses (with suctions of 70 to 80 kPa measured on set-up that generally exceeded the triaxial tests' imposed in situ p'_0 values), incomplete saturation (especially above the water table) and potentially their ≈ 24 times faster strain rates to failure. The UCS strengths also appear ≈ 45% higher than expected from Matthews & Clayton's (1993) correlation with IDD, emphasising the value of site-specific testing.

Next, considering the drainage effects on the saturated 38 mm peak triaxial q_f trends covering in situ p'_0 conditions, the CIU tests (with $s_u = q_f/2$) yield only slightly higher q_f values than the CID tests in shallow Margate Chalk, and inversely in the deeper Seaford. There was minimal undrained pore pressure generation before failure.

CID sample size effects checks showed generally lower q_f and less scattered values for 100 mm than 38 mm dia. specimens, as is often the case for soils with noticeable meso-structure, although the trends showed better convergence at depth due to the tightening and increasing spacing of fissures.

Another aspect examined in Figure 1is the effect of a 300 kPa increase in consolidation pressure. The 'elevated' q_f–depth trend plots ≈ 25% above the 'in situ' series at shallow depth and ≈ 15% above it at greater depth, reflecting the reducing intensity of discontinuities with depth. Consolidation to higher stresses causes gains in 'frictional' strength, albeit with damage to bonding (Liu et al., 2023a). Lastly, the direct simple shear (DSS) s_u trends (taken as peak τ_{vh}) plot consistently ≈ 45% below the CIU triaxial test results, reflecting the chalk's fragile response to tension loading.

4.2 *Stiffness*

Corresponding vertical Young's moduli profiles are provided by Vinck et al. (2022) and identify how drainage condition, sample size, elevated pressures and shearing conditions affect stiffness.

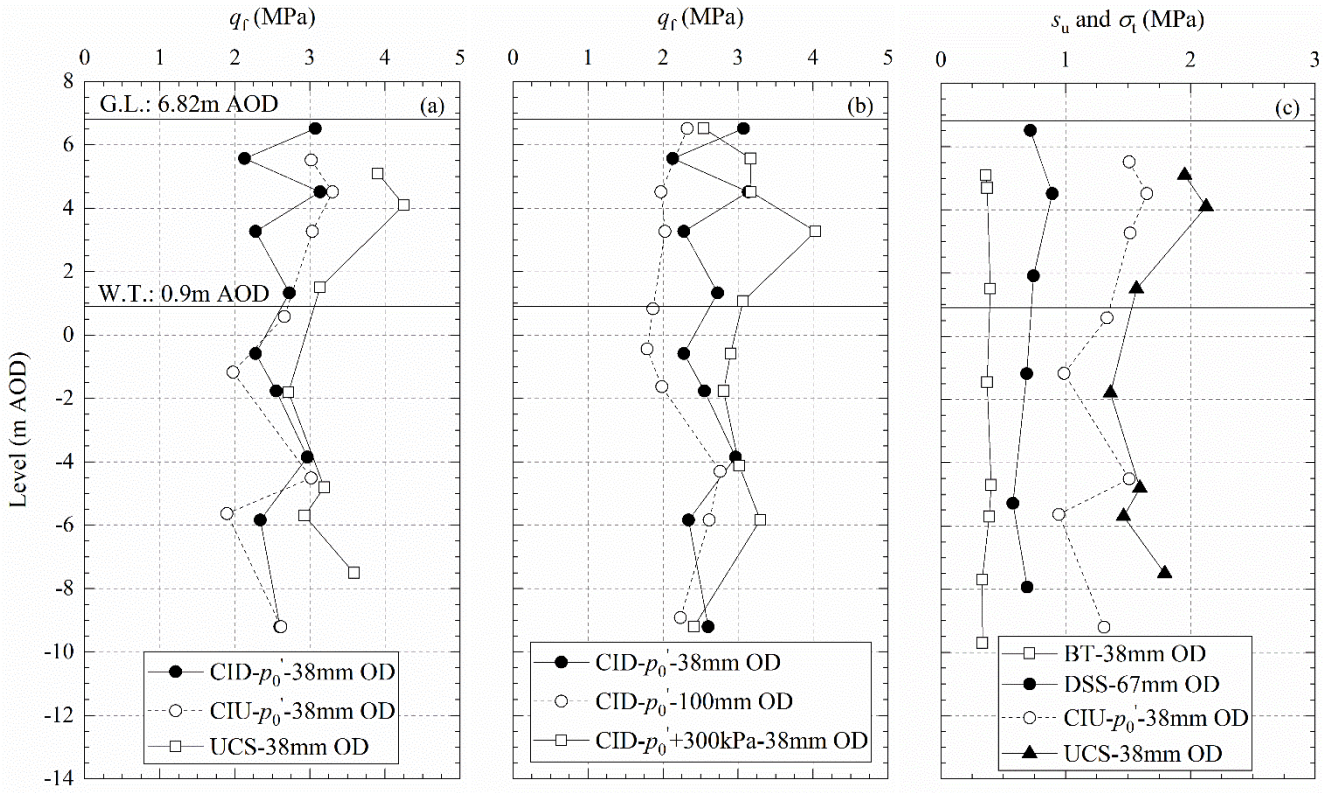

Figure 1: Profiles of peak compressive strength, q_f, considering the effect of drainage condition (a); sample size and elevated pressure (b) and loading condition (c)

The locally instrumented triaxial and UCS moduli are broadly comparable, despite the latter showing more scatter and longer linear ranges. The unusual hierarchy between drained and undrained moduli is

confirmed, with $E'_{v,max}$ exceeding $E^u_{v,max}$ in most cases. Increasing the initial mean effective stress by 300 kPa raised $E'_{v,max}$ by $\approx$ 55% over the first 6 m, but had lesser impact at greater depth. This gain, exceeding that observed for shear strength, is interpreted as the closure of micro- and meso-fissures, more prominent at shallow depths with wider apertures. Notably, the $E'_{v,max}$ of 100 mm dia. triaxial samples exceeds those of smaller specimens, by an average of $\approx$ 45% (excluding one outlier), which may reflect the larger equipment's better stress/strain uniformity and higher resolution measurements.

Figure 2 compares small strain shear stiffnesses offered by various field and laboratory techniques. Profile variations may arise due to specimen disturbance, anisotropy, meso-structure, differing strain rates, variable stress and strain levels, test volumes and instrument resolutions. Comparing laboratory bender element (BE) shear wave velocities with in situ values of the same orientation allows to assess the combined effects of sampling disturbance and meso-fabric to be assessed. While profiles vary across the site, the mean seismic CPT G_{vh} and cross-hole G_{hv} trends fall well below the near-ground-surface triaxial BE G_{vh} measurements, before converging with increasing depth. This trend is interpreted as reflecting the impact of any open fissures, which are systematically avoided when preparing laboratory specimens, occurring less frequently at depth. The DSS G_{vh} maxima fall far below those interpreted from laboratory and field shear wave velocities, confirming the tests' inability to resolve elastic moduli.

Figure 2 also contrasts trends in the cross-hole, BE G_{hh} and pressuremeter G_{hh} (measured at 0·01% shear strain). The BE tests exhibit higher stiffnesses than the seismic field measurements, with laboratory-to-field ratios of 1·1 to 1·5, confirming the systematic impact of meso-structure. Similarly, the pressuremeter data fall well below the geophysical measurements, reflecting the larger-strain behaviour of more disturbed material.

4.3 *Stiffness anisotropy*

The CIU tests' effective stress path inclinations and the systematic trend for initial E_v' to exceed E_v^u indicated that the chalk's vertical moduli exceed equivalent horizontal stiffnesses under in-situ stress conditions. Vinck (2021) explored the anisotropy more precisely through high-resolution BE and monotonic stress probing experiments. Figure 3 presents the profiles with depth of the G_{hh}/G_{vh} ratios found from field (Crosshole, Geotomographie SH-66 sparker) and laboratory tests. Dual axis triaxial BE measurements, made on the same samples, gave $G_{hh}/G_{vh} \approx 0.5$ in the shallow layers and ratios exceeding unity at depth. The G_{hh}/G_{vh} ratios from field seismic tests show a similar, but more muted, trend.

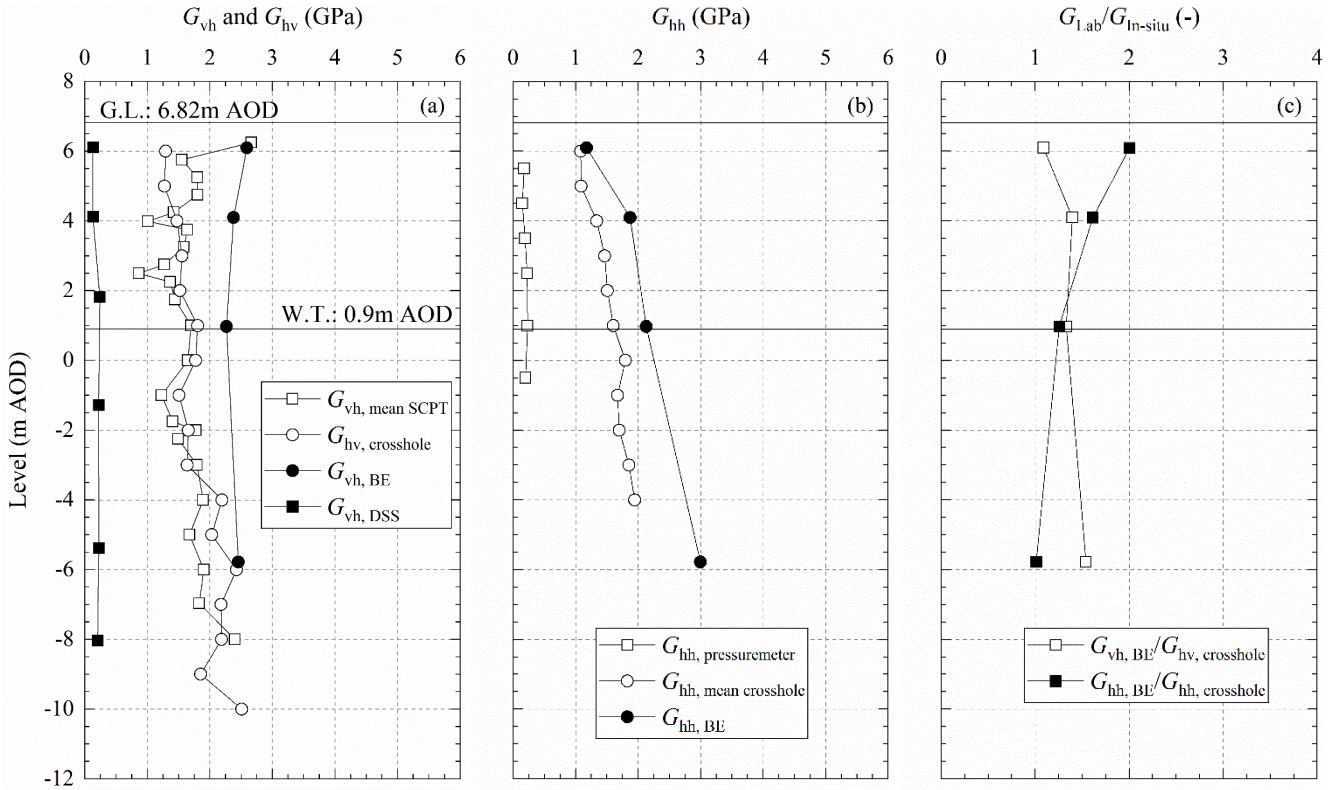

Figure 2: Profiles and ratios of shear stiffness G_{vh} and G_{vh} measured in the lab and in-situ (a) G_{hh} measured in the laboratory and in-situ (b) and with field measurements (c)

Vinck (2021) also conducted small-strain axial and radial drained probes to his triaxial specimens to assess whether their stress-strain behaviour was linear, recoverable, and potentially anisotropic within any Y_1 kinematic yield surface. The axial stress and strain measurements provided easy determination of

vertical stiffnesses. Horizontal stiffness assessment is less direct. Kuwano and Jardine (2002) provide alternative routes for deriving full sets of cross-anisotropic compliance parameters from combined radial probing tests, which define the parameter R in Eq. (1) below and BE G_{hh} measurements. Nevertheless, applying even small radial increments from in-situ stresses resulted in hysteresis and non-uniform responses around the samples' perimeters, indicating the presence of imperfectly closed micro-fissures, predominantly vertical in nature. Treating the chalk as an elastic continuum led to implausible cross-anisotropic υ_{hv}' ratios because the samples' radial behaviour was neither continuous nor fully recoverable, even at very small strains. Vinck (2021) shows that Eqs. (1) and (2) offer the most reliable assessments of horizontal stiffness $E_{h,max}'$, where under axisymmetric triaxial conditions:

$$R = \Delta\sigma_h'/\Delta\varepsilon_h \quad (1)$$

$$E_h' = \frac{4\,R\,G_{hh}}{R+2\,G_{hh}} \quad (2)$$

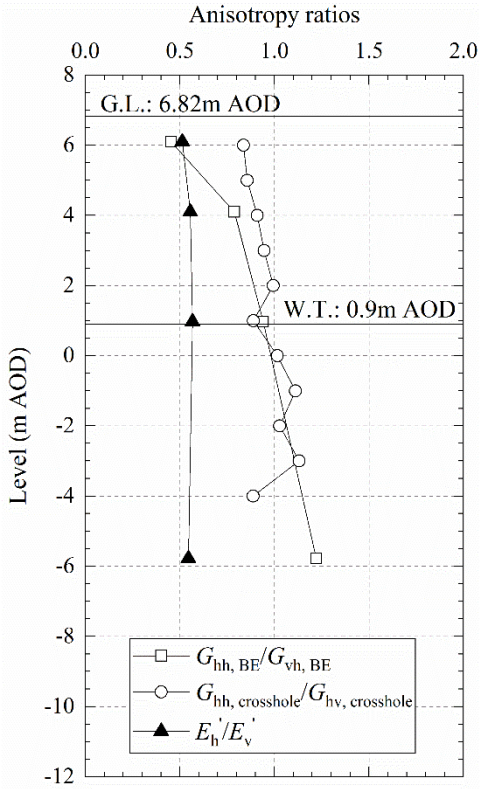

Figure 3: Profiles of stiffness anisotropy as obtained from bender measurements and cross-hole investigations and suites of drained and undrained triaxial probing tests

Figure 2's E_h'/E_v' profile obtained from probing tests confirms that horizontal loading from in-situ stresses provokes a far softer response than vertical compression, a crucial consideration when analysing lateral pile loading. Vinck (2021) shows that anisotropy diminishes after consolidation to higher pressures.

The ALPACA pile tests revealed significantly lower elastic stiffnesses compared to field geophysics and laboratory element tests on intact samples. According to Jardine et al. (2022) and Pedone et al. (2022), this disparity can be attributed to the presence of fissure systems in the chalk mass, which are intentionally avoided during specimen preparation and can be bypassed by geophysical body waves.

5 **Shearing to failure**

5.1 *Shear stress-strain response.*

Vinck et al. (2022) and Liu et al. (2023a) report a series of CID tests with p_0' ranging from 63 kPa to 12.8 MPa. Figure 4 plots their stress-strain responses up to 0.5% axial strain. Y_1 yield points are shown to mark the ends of any initial linear portions. The initial linear stress-strain curves condense into relatively narrow ranges up to ε_a = 0.05%. As discussed later, similar maximum values of vertical stiffnesses E_v' applied in each set, with pressure-dependent Poisson's ratios (υ_{vh}') between 0 and 0.25.

The chalk's response and failure pattern depended markedly on pressure (Figure 5). Tests $p_0' < 363$ kPa reached their peak strengths (q_f) at relatively small strains, with $\varepsilon_a < 0.1\%$, before fracturing and collapsing towards discontinuous assemblies of blocks and fragments. Increasing p_0' from 63 kPa to 1.4 MPa led to disproportionately small increases in q_f and only a 60% gain in peak resistance. However, the degree of brittleness reduced with increasing p_0' and tests with $p_0' > 2$ MPa showed either a ductile or strain hardening response in terms of (q/p').

Tests sheared from in-situ stresses exhibited marked brittleness, characterised by abrupt bond strength loss, discontinuity formation or mobilisation, , and post failure states that deviated from critical states. The latter were only reached with increasing confining pressures under which intact chalk became progressively more ductile and converged towards critical states with $(q/p')_{ult} \approx 1.25$ ($\phi_{cs}' \approx 31°$) (Liu et al. 2023a).

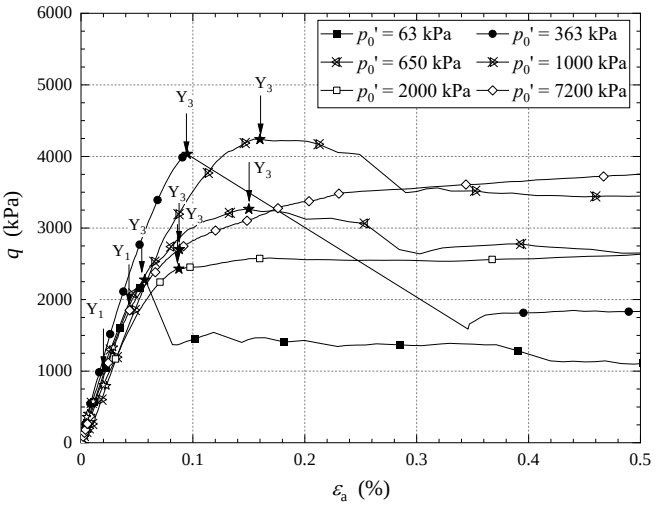

Figure 4: Typical deviatoric stress-axial strain trends over small strain range: 63 kPa < p_0' < 12.8 MPa

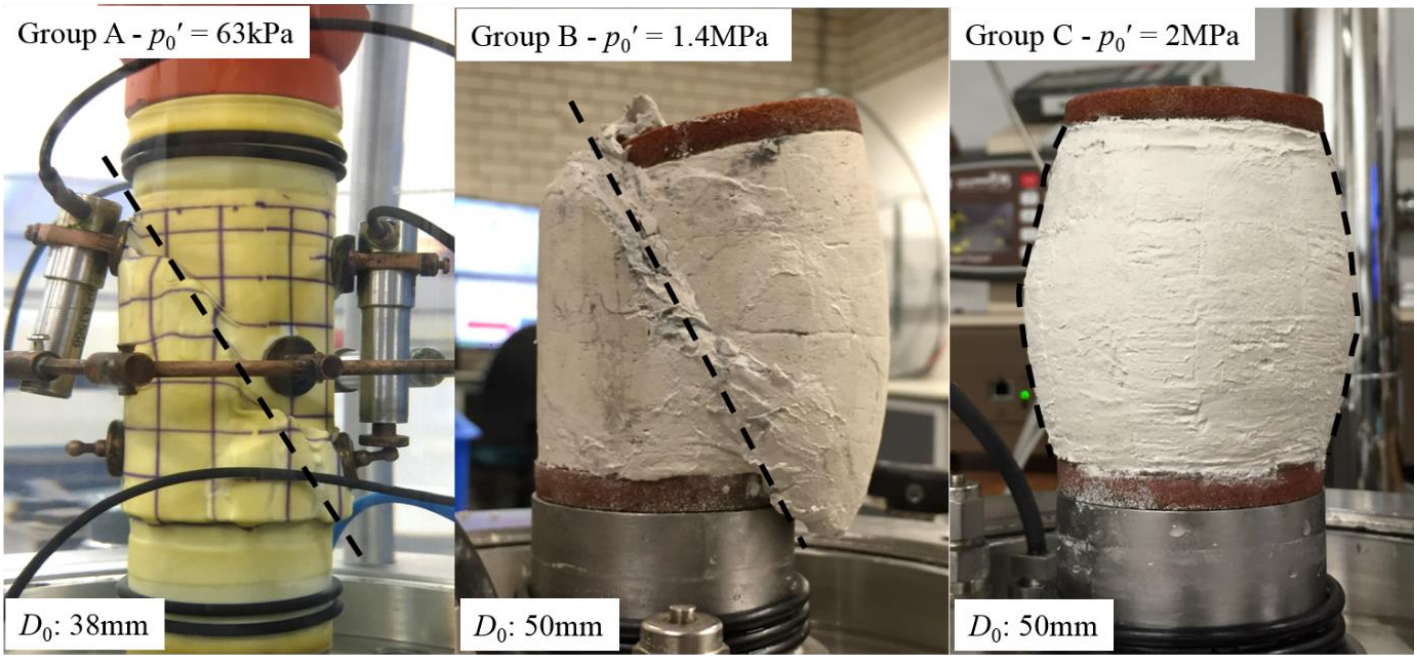

Figure 5: Failure characteristics of intact chalk specimen

5.2 *Volumetric strains*

The shear tests' global volume and axial strain development, as presented in Figure 6, indicate marked changes in dilatancy with increasing p_0'. Tests sheared from in-situ stresses developed minor contractive (positive) volumetric strains (≈ 0.07%) up to their peak strengths, followed by marked 'dilation' as specimens bifurcated and cracked. Similar patterns were reflected in parallel undrained tests' pore pressures (Vinck et al., 2022). Tests with 650 kPa < p_0' < 1.4 MPa exhibited (positive) volumetric strains, following a broad pattern of void ratio reductions increasing with confining pressures, reaching 6% contractive straining after 35% axial strain in the p_0' = 1.4 MPa experiment. The volumetric compressions of tests with 1.4 MPa < p0′ < 12.8 MPa appeared to condense into a narrower range that tended towards volumetric strains of 12-14%. Liu et al. (2023a) further describe the decomposition of the total strains and summarise the plastic axial and volumetric strains as proportions of the corresponding total strains ($\varepsilon_a^p/\varepsilon_a^t$, $\varepsilon_{vol}^p/\varepsilon_{vol}^t$), considering the conditions applying at the Y3 yield points.

Elastic axial straining dominated up to Y_3 yielding in the tests sheared from in-situ stresses. However, dilative plastic volumetric strains were evident from the earliest stages of shearing. This feature probably reflects the systems of partially open micro-fractures and the micro-fissures' closure under higher pressures suppresses this apparently dilative trend, as is common with rocks; Cerfontaine & Collin (2018). The plastic strain components are more important in the higher-pressure tests where they make up, on average, around 42% and 80% of the total axial and volumetric strains at the points of Y_3 yielding, becoming dominant beyond these points.

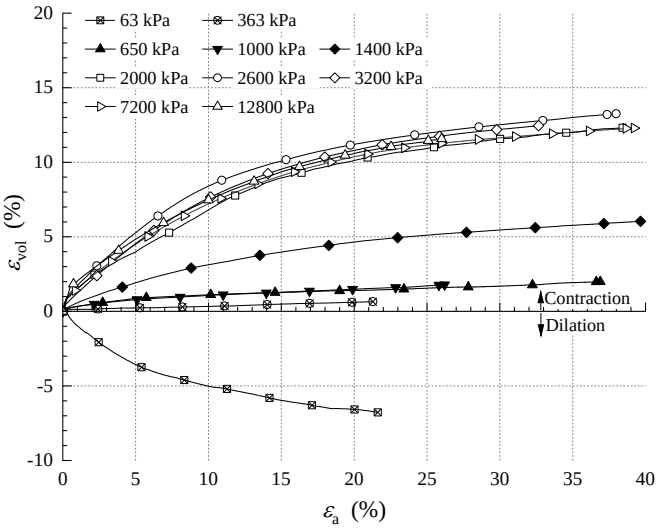

Figure 6: Volumetric strain evolution trends over full axial strain range

5.3 *Peak shear strength*

The chalk's peak strength envelope is curved, leading to shear strength parameters that vary markedly with pressure. Vinck et al. (2022) adopted a pressure-dependent Mohr-Coulomb model to distinguish broadly how intact chalk's 'bonded' and 'frictional' components of strength varied with pressure level. They combined CID and CIU triaxial tests covering 63 kPa < p_0' < 450 kPa to interpret a representative intact peak Mohr-Coulomb envelope with a c' = 490 kPa and ϕ_{peak}' = 39.6° which is re-plotted in Figure 7; other fits apply over different pressure ranges. The lowest p_0' tests developed peak strengths situated marginally to the right of the σ_3' = 0 and q/p' = 3 (no tension) limit that applies in all triaxial tests. The 'low-pressure' tests' relatively high apparent cohesion component reflects the level of inter-particle bonding between the cemented silt-sized calcium carbonate

($CaCO_3$) aggregates, but it is not synonymous with the true component of bonded shear strength, which could not be identified directly from the Authors' experiments.

Increasing p_0' clearly weakens inter-grain bonding and promotes a more 'frictional' shearing response with a curved yield envelope with M ≈ 1.25 or $\phi_{cs}' \approx 31°$ at critical state, implying pressure dependent c′ and ϕ_{peak}' for dry of critical conditions.

While variations between specimens led to a range of low-pressure brittle bifurcation failure patterns, most tended to form shear zones inclined at 60-65° to the horizontal. The 'high pressure' ductile specimens formed bulging failures and delivered markedly reduced post-test water contents (16-23%), while 'elevated pressure' specimens developed both radial bulging and formed 6-8 mm thick bands of remoulded chalk within diffused shear zones inclined ≈65° to the horizontal (Figure 5).

The peak triaxial compressive shear strengths of bonded weak rocks are relatively insensitive to consolidation paths applied within their Y_3 envelopes (Leroueil & Vaughan 1990). They generally offer far lower strengths in tension. Figure 1 confirms that far lower shear strengths and stiffness apply to chalk in tests that induce tensile failure. Their Brazilian tension (BT) strengths were 90% lower than the UCS values, while the DSS strengths were 50% lower than those mobilised in triaxial compression.

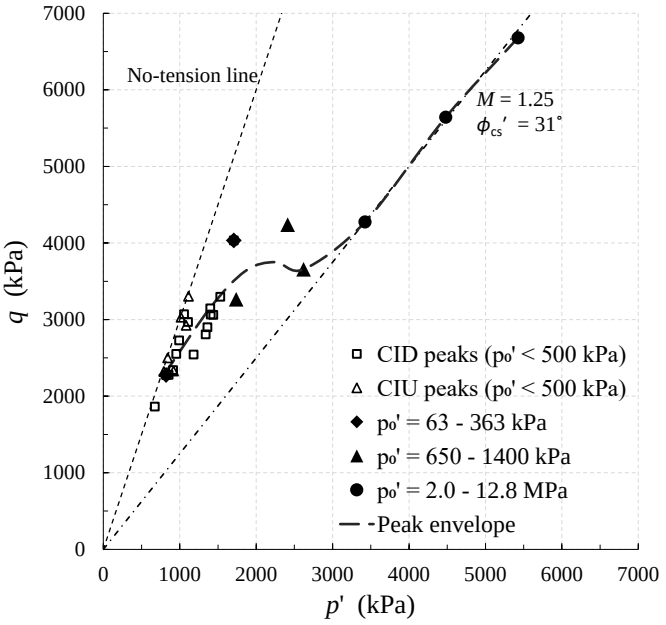

Figure 7: Peak and ultimate shear strength envelope for intact chalk

6 **Conclusions**

This paper summarises the key outcomes from comprehensive in-situ and laboratory testing on intact low- to medium-density chalk conducted for the ALPACA JIPs to aid the interpretation of axial and lateral pile load tests. The key conclusions drawn are:

(1) Intact chalk exists at states it cannot sustain when reconstituted. It is highly sensitive and de-structures when taken to large strains.
(2) De-structuration and tensile failure affect the responses seen in field and laboratory shear tests.
(3) A clear hierarchy exists between strengths obtained from UCS, triaxial, DSS and BT tests.
(4) The chalk's behaviour is markedly pressure dependent. When loaded from in-situ p_0' conditions, it manifests remarkably brittle, bonded behaviour after relatively small axial strains (≈0.15%) with apparent cohesion components that contribute a large proportion of their peak deviator stresses. However, this decays rapidly post-peak.
(5) Raising the initial isotropic p_0' levels into the MPa range leads to ductile behaviour and compressive volumetric straining. All experiments conducted with $p_0' \geq 650$ kPa tended towards final critical states with M = 1.25, equivalent to $\phi' \approx 31°$.
(6) Specimen failure patterns also evolve from showing discontinuous bifurcation after small axial strains (≈ 0.1%) to bulging and peak resistances developing after large (≈ 40%) strains.
(7) Drained isotropic loading invokes tangent bulk moduli K′ that initially increase until micro-fissures close fully, after which K′ remains high and practically constant until large strain yielding commences and sharp K′ reductions occur.
(8) The chalk also shows very stiff initial near linear shearing behaviour. Vertical Young's moduli E_v' increase modestly with pressure until they manifest their maximum (7.7 GPa) at moderate pressures (with $p_0' = 650$ kPa) before falling to a 4 MPa minimum plateau. This behaviour differs strikingly from that of unbonded geomaterials.
(9) CID and CIU triaxial compression tests sheared from in situ stresses developed closely similar effective stress paths inclinations reflecting marked stiffness anisotropy, with $E_h'/E_v' < 1$ due to open micro-fissures. Samples consolidated to pressures that close these fissures show far less anisotropy. Field geophysical tests reveal similar patterns for $G_{hh}'/G_{hv}' < 1$.
(10) Meso-to-macro systems of fissuring lead to field axial and lateral pile loading experiments showing far lower elastic stiffnesses than either field geophysical, or locally instrumented triaxial tests on intact specimens.

Acknowledgments

The study was carried out as part of the ALPACA project funded by the Engineering and Physical Science Research Council (EPSRC) grant EP/P033091/1, Royal Society Newton Advanced Fellowship NA160438 and Supergen ORE Hub 2018 (EPSRC EP/S000747/1). Byrne is supported by the Royal Academy of Engineering under the Re-search Chairs and Senior Research Fellowships scheme. The authors acknowledge additional financial and technical support by Atkins, Cathie Associates, Equinor, Fugro, Geotechnical Consulting Group (GCG), Iberdrola, Innogy, LEMS, Ørsted, Parkwind, Siemens, TATA Steel and Vattenfall. Imperial College's EPSRC Centre for Doctoral Training (CDT) in Sustainable Civil Engineering and the DEME Group (Belgium) supported Ken Vinck. Socotec UK Ltd and Fugro carried out the block sampling and rotary core sampling campaigns. Technical support from Ben Boorman and Matt Wilkinson (University College London) and Steve Ackerley, Graham Keefe, Prash Hirani, Stef Karapanagiotidis, Graham Nash, Gary Jones (Imperial College London) is greatly acknowledged.

References

Ahmadi-Naghadeh R., Liu T, Vinck K, Jardine RJ, Kontoe S, Byrne BW, McAdam RA. (2022). Laboratory characterisation of the response of intact chalk to cyclic loading. Ahead of Print in Géotechnique, 2022. https://doi.org/10.1680/jgeot.21.00198

ASTM International. D4543-19. (2019). Standard Practices for Preparing Rock Core as Cylindrical Test Specimens and Verifying Conformance to Dimensional and Shape Tolerances. West Conshohocken, PA; ASTM International. https://doi.org/10.1520/D4543-19

Barbosa PM., Geduhn M, Jardine RJ, Schroeder FC. (2017). Large scale offshore static pile tests-practicality and benefits. Society for Underwater Technology: 8th International Conference on Offshore Site Investigation and Geotechnics, Smarter Solutions for Offshore Developments, London, UK, vol. 1, 644-651, 2017.

Buckley RM, Jardine RJ, Kontoe S, Barbosa P and Schroeder FC. (2020). Full-scale observations of dynamic and static axial responses of offshore piles driven in chalk and tills. Géotechnique,70 (8), pp. 657-681. https://doi.org/10.1680/jgeot.19.TI.001

Cerfontaine B and Collin F. (2018). Cyclic and fatigue behaviour of rock materials: Review, interpretation and research perspectives. Rock Mech Rock Eng 51, 391–414. https://doi.org/10.1007/s00603-017-1337-5

Jardine RJ, Buckley RM, Liu T, Byrne BW, Kontoe S, McAdam RA, Schranz F and Vinck K. (2023a). Driven pile behaviour in low-to-medium density chalk: the ALPACA JIP outcomes. Submitted to 9th Int. Conf. on Offshore Site Investigations and Geotechnics, SUT London.

Jardine RJ, Buckley RM, Liu T, Andolfsson T, Byrne BW, Kontoe S, McAdam RA, Schranz F and Vinck K (2023b). The axial behaviour of piles driven in chalk. Géotechnique. Ahead of Print https://doi.org/10.1680/jgeot.22.00041

Kuwano R, Jardine RJ. (2002). On the applicability of cross-anisotropic elasticity to granular materials at very small strains. Géotechnique, 52(10):727-749. https://doi.org/10.1680/geot.2002.52.10.727

Leroueil S and Vaughan PR. (1990). The general and congruent effects of structure in natural soils and weak rocks. Géotechnique, 40(3):467-488. https://doi.org/10.1680/geot.1990.40.3.467

Liu T, Ahmadi-Naghadeh R, Vinck K, Jardine RJ, Kontoe S, Buckley RM, Byrne BW. (2022). An experimental investigation into the behaviour of de-structured chalk under cyclic loading. Ahead of Print in Géotechnique, 2022. https://doi.org/10.1680/jgeot.21.00199

Liu T, Ferreira PMV, Vinck K, Coop MR, Jardine RJ, Kontoe S. (2023a). The behaviour of a low-to-medium density chalk under a wide range of pressure conditions. Soils and Foundations, 63(1). https://doi.org/10.1016/j.sandf.2022.101268

Liu T, Jardine RJ, Vinck K., Ahmadi-Naghadeh R, Kontoe S, Buckley RM, Byrne BW, McAdam RA. (2023b). Cyclic characterisation of low-to-medium density chalk for offshore driven pile design. Submitted to Offshore Site Investigation and Geotechnics Conference, Society of Underwater Technology, London, UK.

Lord JA, Clayton CRI and Mortimore RN. (2002). Engineering in chalk, C574. London, UK: CIRIA.

Matthews MC and Clayton CRI. (1993). Influence of intact porosity on the engineering properties of a weak rock. In Proceedings of the 1st international symposium on geotechnical engineering of hard soils–soft rocks (eds A. Anagnostopoulos, F. Schosser, N. Kalteziotis and R. Frank), pp. 693–702. Rotterdam, the Netherlands: Balkema.

McAdam RA, Buckley RM, Schranz F, Byrne BW, Jardine RJ, Kontoe S, Liu T, Vinck K, Crispin J. (2023). Monotonic and cyclic lateral loading of piles in low to medium density chalk, 2022. Géotechnique Under review.

Mortimore RN. (2012). The 11th Glossop Lecture: Making sense of chalk: a total-rock approach to its engineering geology. Q. J. Engng Geol. Hydrogeol. 45, No. 3, 252–334. https://doi.org/10.1144/1470-9236/11-052.

Pedone G, Kontoe S, Zdravković L, Jardine RJ, Vinck K, Liu T. (2023). Numerical modelling of laterally loaded piles driven in low-to-medium density fractured chalk. Computers and Geotechnics, Volume 156. https://doi.org/10.1016/j.compgeo.2023.105252

Skempton AW. (1954). The pore-pressure coefficients A and B. Géotechnique 4, No. 4, 143–147. https://doi.org/10.1680/geot.1954.4.4.143.

Vinck K. (2021). Advanced geotechnical characterisation to support driven pile design at chalk sites. PhD thesis, Department of Civil and Environmental Engineering, Imperial College London.

Vinck K., Liu T, Jardine RJ, Kontoe S, Ahmadi-Naghadeh R, Buckley RM, Byrne BW, Lawrence JA, McAdam RA, Schranz F. (2022). Advanced in situ and laboratory characterization of the ALPACA chalk research site. Ahead of Print in Géotechnique. https://doi.org/10.1680/jgeot.21.00197